Bistatic 3D SAR for wall parameter extraction in cluttered environments

James Elgy,[1,✉] Daniel Andre,[1] and Mark Finnis[2]
[1]*Defence Academy of the United Kingdom, Centre for Electronic Warfare, Information, and CyberCranfield University, Shrivenham, UK*
[2]*Centre for Defence Engineering, Defence Academy of the United Kingdom, Cranfield University, Shrivenham, UK*
✉Email: James.D.Elgy@Cranfield.ac.uk

Through-wall radar is an emergent technology rooted in urban surveillance, a key component being synthetic aperture radar (SAR). Accurate through-wall SAR relies on knowledge of the refractive index and thickness of any obscuring walls. Such information is rarely known beforehand and is subject to change on a sample-by-sample basis. It is therefore necessary to obtain the material properties in conjunction with any SAR measurement. In this letter, a remote data-driven asymmetric bistatic SAR approach is taken by means of matching the range to the direct back face reflection with an explicit geometry-based model. The proposed method relies on an accurate knowledge of the bistatic measurement geometry. Using the bright reflection from the front face of the wall, a method for refining an estimate of the bistatic measurement geometry is proposed. This approach is extended to three-dimensions to improve usability in heavily cluttered environments. This method is empirically validated using three-dimensional SAR measurements of both a wall-only, and a heavily cluttered scene. The method is shown to accurately extract both the refractive index and thickness of a concrete wall, with both measurements in agreement with each other and an independent validation measurement.

Introduction: Accurate through-wall synthetic aperture radar (SAR) relies on an accurate estimation of the electrical properties of any obscuring wall. In particular, knowledge of the material's refractive index, n, and thickness, δ, are required. In practice, however, the properties of building materials are rarely known a priori and can vary substantially between samples. It is therefore necessary to obtain the properties of any walls on a per case basis.

Methods for obtaining both the thickness and refractive index of a wall broadly fall within three categories: auto-focus-based optimisation [1, 2], direct reflectivity measurements [3, 4], and bistatic separation measurements between the wall front and back face scattering responses [5–8]. There are limitations to each of these approaches. The auto-focus optimisation is ill-posed for heavily cluttered measurements, due to the interaction of multiple point spread functions and wall signatures. Direct reflectivity measurements require a comprehensive calibration of the radar system, and the introduction of a highly reflective reference object, usually a metal plate. For these reasons, these methods are problematic for application to real-world scenarios. While there are experimental examples of each approach, these are often idealistic with regards to the measurement geometry and scene clutter content. For this reason, it would be beneficial to have an approach applicable to scenarios with heavily cluttered environments. Measuring the separation between faces has shown promising clutter rejection properties when used in conjunction with two-dimensional bistatic SAR measurements [7]. In this letter, this method is extended into a three-dimensional scenario to allow more definitive clutter rejection, by providing a greater sampling of the wall structure and providing the elevation resolution required to separate the clutter from the wall signature of interest.

Asymmetric Bistatic Model: To form accurate SAR images, both the refractive index and thickness of the wall must be determined; for this, the front and back face wall signatures are required. In the method presented here, an asymmetric bistatic SAR collection approach is employed for this, which in addition to allowing the determination of the parameters, will also allow SAR image formation with the same data.

Since the angle of incidence, and by extension the range separation between faces varies as a function of bistatic antenna positioning, it is necessary to construct a model for the propagation through the material. Consider a bistatic configuration consisting of a transmitting antenna, $T = [T_x, T_y, T_z]$, a distance D from a wall of thickness δ and an independent receiving antenna, $R = [R_x, R_y, R_z]$. The relation between the antennas is defined by the bistatic baseline vector $V = R - T$ as illustrated in Figure 1. The bistatic range to the front face of the wall, R_{front}, is computed via knowledge of the distance to the wall, and the bistatic baseline vector:

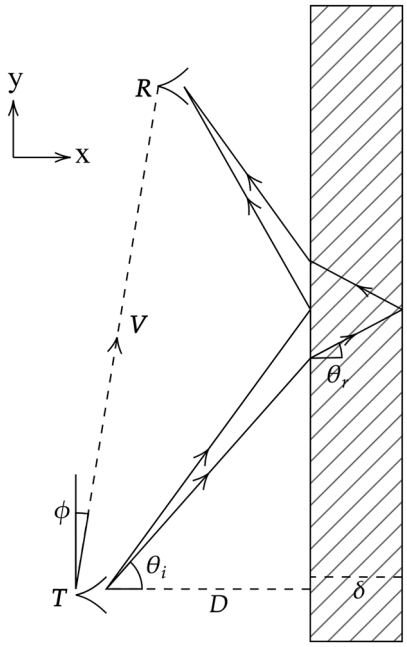

Fig. 1 *Diagram showing the asymmetric bistatic geometry and the associated refracted path. The refracted paths scattered from the front and back wall faces,with respective ranges* R_{front} *and* R_{back}*, are shown in the* X–Y *plane*

$$R_{front} = \sqrt{V_y^2 + (2D - V_x)^2 + V_z^2} \tag{1}$$

where V_x, V_y and V_z are the components of $\boldsymbol{V}$. The range to the back face, R_{back}, is dependent upon both the wall thickness and refractive index, and for a given pair of parameters, is obtained via:

$$R_{back} = \frac{2D - V_x}{\cos(\theta_i)} + \frac{2n\delta}{\cos(\theta_r)} \tag{2}$$

$$\theta_i = \operatorname{argmin}\left(\left|(2D - V_x)\tan(\theta_i) + 2\delta\tan(\theta_r) - V_y\right|\right) \tag{3}$$

where θ_i represents the angle of incidence and θ_r represents the associated angle of refraction. The relation between them is defined by Snell's Law.

Equation (2) is extended to three dimensions by noting that the point of reflection must lie on the plane containing the two antenna positions and is also perpendicular to the wall, thus the two-dimensional representation given by Figure 1 is obtained by rotation around the x-axis.

Obtaining Bistatic Geometry: For a SAR measurement, the bistatic geometry with respect to the wall may not be known to a suitable precision. For the extraction of the wall properties to be effective, the bistatic geometry of the collection with respect to the wall must be accurately known; in particular, the angle of the wall with respect to the collection must be known. Extensive simulations have found that uncertainty in $\boldsymbol{V}$ greater than 1 cm results in significant uncertainties associated with the extracted values [7]. Since it is often not possible to approach the wall structure, a data-based approach to finding the geometry is preferable. For a SAR collection consisting of p pulses, the subscript l denotes the index for the pulse such that $l = 1, 2, 3 \ldots p$. Since there are multiple variables that must be obtained, $\boldsymbol{V}_l$, D_l, and the angle of the wall with respect to the SAR system φ_l, multiple bistatic geometries are required for this approach. For a known SAR trajectory, the geometry of the system with respect to the wall can be reconstructed from the geometry of the first position, $\boldsymbol{V}_1$, D_1, and the wall angle with respect to $\boldsymbol{V}_1$

Fig. 2 *Photograph of the cluttered scene, showing two metal drums, a bicycle, a metal briefcase, a desk, a desktop computer, and a computer monitor*

Since the wall acts as a constant bright reflector, and the range to the front face of the wall can be evaluated via Equation (1), refining an initial estimation of the bistatic geometry based on the measured data is possible. Given that the front face signature is consistently bright across the synthetic aperture, obtaining the range to the front face signature for a given bistatic geometry is achieved via finding the first brightest peak, R_{peak}, in the l^{th} range-profile, $\rho(r, l)$ where r represents range:

$$R_{peak_l} = \operatorname{argmax}\left(\rho\left(r,\ l\right)\right) \tag{4}$$

where $l = 1, 2, 3 \ldots p$. Matching the measurement data to the theoretical model (Equation 1) is achieved via a non-linear least-squares approach:

$$\boldsymbol{S} = \operatorname{argmin}\left(\sum_{l=1}^{p}\left|R_{peak_l} - R_{front_l}\right|^2\right) \tag{5}$$

$$\boldsymbol{S} = \left[V_1,\ D_1,\ \phi\right] \tag{6}$$

Refining the bistatic geometry based on both an initial estimation of the geometry and the measured data has provided significantly improved parameter extraction capability [7] when compared to manually measuring the geometry [6].

Parameter Extraction: The values for refractive index and thickness are obtained by fitting Equations (1) and (2) to measured radar scan data. This consists of a sequence of bistatic range-profiles $\rho(r,l)$, r denoting range and l denoting the lth range-profile. In this sequence of profiles, the separation between the wall front and back-faces will be seen to vary. To simplify the process, range-profiles are aligned so that the front face response occurs at 0 m for all profiles. In the fitting process, the cost function $F(n, \delta)$ is employed and is a sum over range-profile intensities at the model's predicted wall back-face signature location in the range:

$$F\ (n, \delta) = \sum_{l=1}^{p}\left|\rho\left(R_{back}\left(n, \delta, D_l, \boldsymbol{V}_l\right) - R_{front}\left(D_l,\ \boldsymbol{V}_l\right),\ l\right)\right|^2 \tag{7}$$

$$(n, \delta) = \operatorname{argmax}\left(F\left(n, \delta\right)\right) \tag{8}$$

Experimental Validation: Validation of the proposed approach has been performed using experimental data gathered at Cranfield University's GBSAR facility. The system consists of a motorised vertical arm suspended from a horizontal gantry. Two identical antennas are connected to a vector network analyser from which a chirp pulse is generated.

Two scenarios are compared. The first being a 'wall only' scenario, where no additional scatterers are added. The second scenario is a heavily cluttered scene, pictured in Figure 2. This scene consists of two metal barrels, a metal briefcase, a desk, a computer monitor, a desktop computer, and a bicycle, all placed immediately behind the wall.

In both scenarios, a wall consisting of Cemex 1400 lightweight concrete aggregate blocks is constructed 3.64 m from the SAR system. This distance is sufficient to separate in range the direct antenna coupling signature and the signatures of interest.

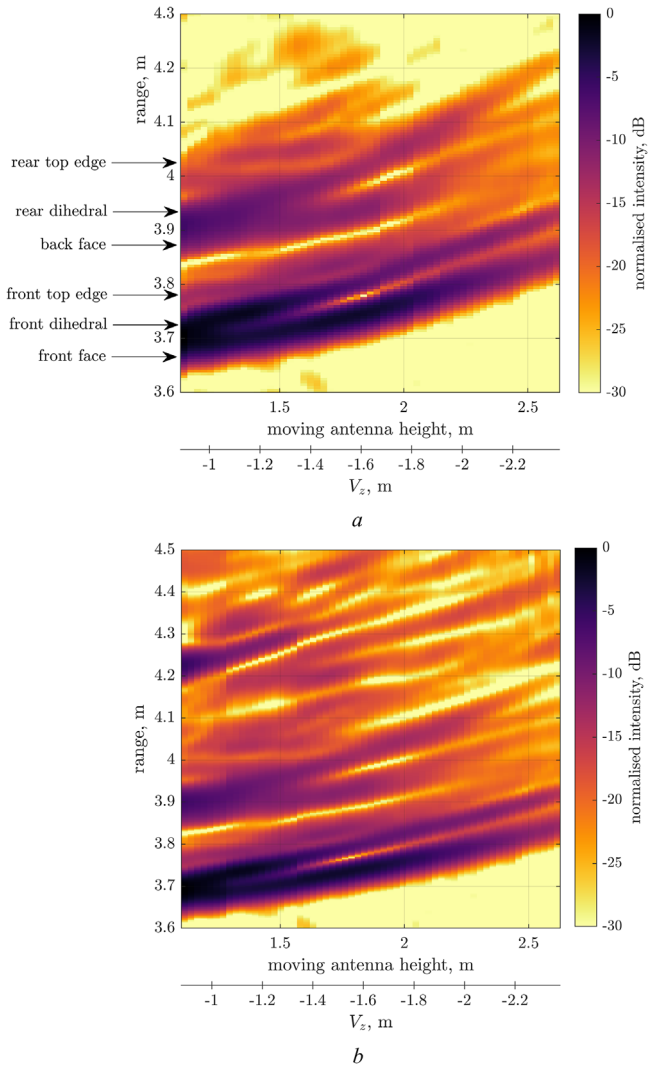

Fig. 3 *Evolution of the wall signature with height for both: (a) Non-cluttered measurement. (b) cluttered measurement*

The bistatic geometry consists of a stationary antenna mounted on a polystyrene plinth and a moving antenna traversing a 3.5 m by 1.5 m vertical rectangular aperture in 2.5 cm increments, resulting in 8601 pulses of 5 GHz bandwidth, from 1 GHz to 6 GHz. The bistatic geometry of the collection was maintained for the two measurements.

The refractive index and thickness properties of the wall were independently obtained using a digital calliper and direct range measurements of an obscured and non-obscured trihedral. From these measurements, the wall properties for the concrete wall under test are known to be: $n = 2.26 \pm 5.5\%$ and $\delta = 9.66 \pm 0.3\%$ cm [7].

Figure 3 shows the evolution of the measured range-profile data with height, for the two scenarios. This highlights the difficulty with separating the clutter from the wall signature. This is again illustrated in the 3D-SAR imagery in Figures 4 and 5 where the clutter immediately behind the wall, in particular the desk, computer monitor and bicycle, are shown to overlap with the wall signature. In addition, the background multipath is present in both images. For this reason, auto-focus-based approaches may be ill-suited for this type of measurement.

From the height evolution presented in Figure 3, the back-face signature is seen to overlap with the dihedral signature formed at the intersection between the wall and the floor. In particular, the rear dihedral formed between the ground and the rear face of the wall and the dihedral signature formed by the top edge of the wall structure are similar in range to the direct specular reflection from the back face of the wall. For this reason, the lower antenna heights should not be used to find the wall properties.

Using the top height range of 0.7 m (4000 pulses) results in the extracted results presented in Table 1. Error bars have been established

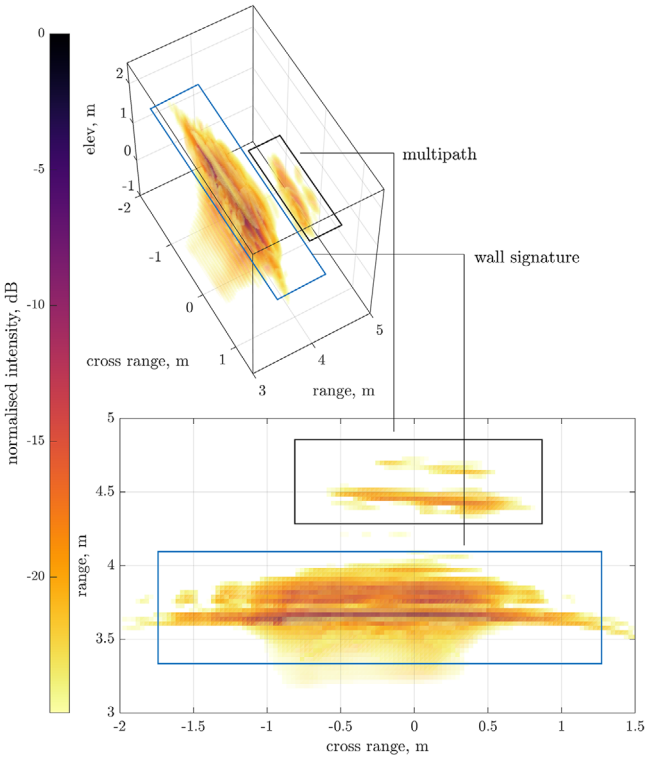

Fig. 4 *Refraction corrected SAR image for the wall-only measurement*

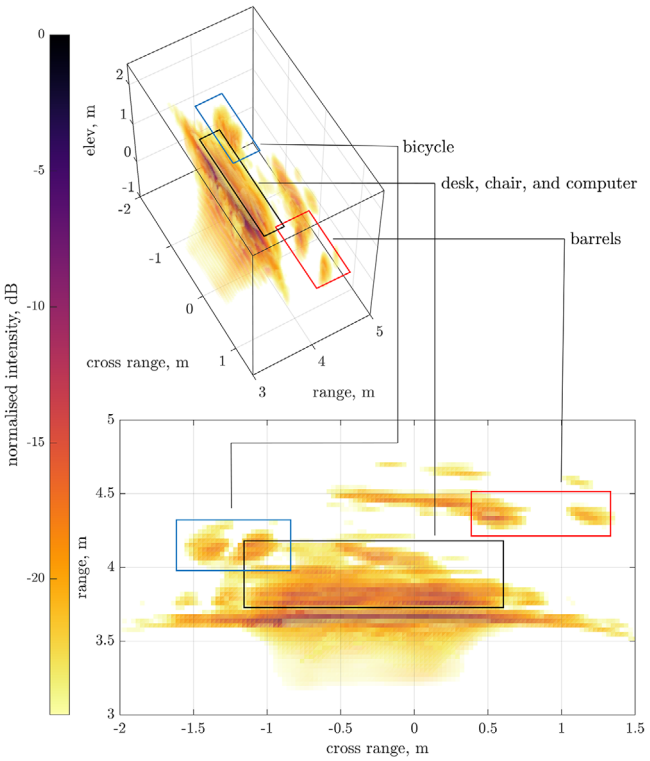

Fig. 5 *Refraction compensated bistatic SAR image for the cluttered measurement. In addition to the wall signature and multipath shown in Figure 4, the clutter is shown to overlap with the wall signature, in particular, the desk, chair and computer. This makes auto-focus based approaches unsuitable for this measurement*

Table 1. Extracted refractive index and thickness for cluttered and non-cluttered measurements

	n	δ (mm)
True value	2.26 ± 0.12	96.6 ± 0.29
No scene	2.23 ± 0.31	98.5 ± 9.85
With scene	2.31 ± 0.32	95.0 ± 9.50

by evaluating a simulation of the wall and systematically introducing uncertainties into the assumed geometry, noise level, and material imperfections [7]. For the bandwidth and SAR system used in these tests, the error bars associated with the refractive index and thickness are estimated to be 14% and 10% respectively. This is sufficient to establish that both scenarios produce results that agree with each other and with the validation measurements performed beforehand as well as the two-dimensional SAR measurements performed in [7].

Conclusion: In this letter, a natural development of the two-dimensional parameter extraction methodology [3, 5, 8] is employed. This new generalised approach has the benefit of further mitigating both clutter, and multipath effects via multiple radar heights. This height variation allows for the alleviation of overlapping wall-ground dihedral and clutter signatures via judicious vertical sub-aperture selection.

Two scenarios are considered; a cluttered and a non-cluttered environment, both measured using the same wall material and radar geometry. The extracted refractive index and thickness of the concrete material agree with both scenarios and with an independent validation measurement. It has been demonstrated that significant clutter does not impede the accurate extraction of the wall properties. Moreover, this is demonstrated without the need for background measurements. Furthermore, imprecise measurements of the bistatic geometry can be overcome via a data-driven approach involving the front face wall reflection in relation to the established model.

Future investigation should focus on further generalisation of the bistatic geometry. For example, a small drone swarm would provide greater flexibility than a static system and allow investigations of diverse geometries and sample rates.

Acknowledgements: This work was supported by Defence Science and Technology Laboratory (Dstl). Furthermore, the authors would like to thank Cemex UK for the donation of the concrete blocks used throughout this work.

© 2021 The Authors. *Electronics Letters* published by John Wiley & Sons Ltd on behalf of The Institution of Engineering and Technology

This is an open access article under the terms of the Creative Commons Attribution License, which permits use, distribution and reproduction in any medium, provided the original work is properly cited.
Received: *6 June 2021* Accepted: *26 June 2021*
doi: 10.1049/ell2.12273

References

1 Khorashadi-Zadeh, V., Dehmollaian, M.: Through a cinder block wall refocusing using SAR back projection method. *IEEE Trans. Antennas Propag.* **67**(2), 1212–1222 (2019) https://doi.org/10.1109/TAP.2018.2882599
2 Jin, T., et al.: Image-domain estimation of wall parameters for autofocusing of through-the-wall SAR imagery. *IEEE Trans. Geosci. Remote Sens.* **51**(3), 1836–1843 (2013) https://doi.org/10.1109/TGRS.2012.2206395
3 Thajudeen, C., Hoorfar, A.: Wall parameters estimation using a hybrid time-delay-only and reflected wave ratio technique. In: IEEE Antennas and Propagation Society International Symposium (APSURSI), Orlando, FL, USA, 7–13 July 2013 https://doi.org/10.1029/2010RS004631.M
4 Aftanas, M., et al.: Efficient and fast method of wall parameter estimation by using UWB radar system. *Frequenz* **63**(11–12), 231–235 (2009) https://doi.org/10.1515/FREQ.2009.63.11-12.231
5 Thajudeen, C., Hoorfar, A.: A hybrid bistatic-monostatic radar technique for calibration-free estimation of lossy wall parameters. *IEEE Antennas Wirel. Propag. Lett.* **16**, 1249–1252 (2017) https://doi.org/10.1109/LAWP.2016.2630006
6 Elgy, J., et al.: Data driven corrections to multistatic 3D through-wall radar imagery," In: Proceedings of the Institute of Acoustics, Lerici, Italy, vol. 40 part 2, pp. 199–208 (2018).
7 Elgy, J.: Bistatic SAR for building wall material characterisation. PhD Thesis, Cranfield University, (2021)
8 Protiva, P., et al.: Estimation of wall parameters from time-delay-only through-wall radar measurements. *IEEE Trans. Antennas Propag.* **59**(11), 4268–4278 (2011) https://doi.org/10.1109/TAP.2011.2164206

https://dspace.org/

Bistatic 3D SAR for wall parameter extraction in cluttered environments

Elgy, James; Andre, Daniel; Finnis, Mark V.

2021-07-28
Institution of Engineering and Technology (IET)
https://doi.org/10.1049/ell2.12273
Elgy J, Andre D, Finnis M. (2021) Bistatic 3D SAR for wall parameter extraction in cluttered environments. Electronics Letters, Volume 57, Issue 21, October 2021, pp. 807-809

Downloaded from a DSpace repository. https://dspace.org/